Food Bioprocess Technol (2015) 8:777–790
DOI 10.1007/s11947-014-1445-0

ORIGINAL PAPER

Temperature-Associated Proton Dynamics in Wheat Starch-Based Model Systems and Wheat Flour Dough Evaluated by NMR

C. Rondeau-Mouro · M. Cambert · R. Kovrlija · M. Musse · T. Lucas · F. Mariette

Received: 24 July 2014 / Accepted: 20 November 2014 / Published online: 30 November 2014

Abstract Wheat starch-based model systems and wheat flour dough with the same water content (close to 45 %) were investigated upon heating (20–90 °C) using time-domain ^{1}H NMR spectroscopy with the aim of assigning each spin–spin relaxation time (T_2) measured to a specific proton fraction. On the basis of the signal evolution according to Curie's law for pure starch and pure water, temperature-associated changes for each T_2 value and their mass intensity were interpreted and assigned to water and/or biopolymer proton fractions related to the reversible swelling of starch or its gelatinization. The addition of 2 % (*w*/*w*) salt to model samples and dough induced few changes during the reversible swelling process but impacted on the measurements performed above 60 °C. Finally, studies performed on starch-based model systems improved understanding of the complex thermal processing of starch in dough by taking into account phenomena other than the starch swelling and gelatinization, such as gluten denaturation and changes in water–biopolymer interactions.

Keywords TD-NMR · Low-field NMR · Relaxation · ANOVA · Swelling · Gelatinization · Bread

Introduction

Starch swelling and gelatinization are transition processes occurring upon hydration and heating of starch granules (Biliaderis 1992; Donald 2004). Gelatinization followed by a cooling process contributes to the crumb structure and the textural properties of many cereal products (Wilhoft 1973). Gelatinization transition is a nonequilibrium process resulting from the diffusion of water into the starch granules, their hydration, and reversible swelling, while the uptake of heat induces an irreversible swelling of granules which lose their crystallinity and structural organization. While water diffuses into granules, water molecules interact by hydrogen bonding to the exposed hydroxyl groups of amylose and amylopectin. This starch swelling phenomenon is accompanied by leaching of granule constituents, predominantly amylose (Steeneken 1989; Leach et al. 1961). This ability to interact with water is not uniform within the starch granule, due to the heterogeneous distribution of water into granules and their semicrystalline nature (Ollett et al. 1993). The gelatinization process occurs initially in the amorphous regions, as opposed to the crystalline regions of the granule, a consequence of supposed weakened hydrogen bonding in these areas. When the temperature is high enough (close to 60 °C), the granules become increasingly susceptible to shear disintegration as they swell, and they release materials such as amylose and destructured amylopectin as they disintegrate. Further heating over 80 °C and stirring lead to the total disintegration of the granule structure, solubilization of the starch, and decrease in viscosity. Without stirring, the hot starch paste is a mixture of fragments of swollen granules and colloidally and molecularly dispersed starch granules (Donald 2004).

Based on spin–spin T_2 relaxation time measurements, time-domain NMR spectroscopy (TD-NMR) has been shown to provide reliable information on the water and biopolymer mobility, especially in starch-based systems. However, no studies have involved temperature dynamics investigations (upon heating) of wheat starch-based model systems of high water content (>35 %). TD-NMR studies have instead been performed on hydrated starches of other origins (rice, potatoes, peas, etc.) upon heating (Tang et al. 2001; Fan et al.

C. Rondeau-Mouro (✉) · M. Cambert · R. Kovrlija · M. Musse · T. Lucas · F. Mariette
IRM-Food , UR TERE, IRSTEA, CS 64426, 17 Avenue de Cucillé, 35044 Rennes Cedex, France
e-mail: corinne.rondeau@irstea.fr

2013; Ritota et al. 2008; Tananuwong and Reid 2004) or on more complex recipes based on wheat starch but of low water content (16–23 %) together with other ingredients (sugar and fat) (Assifaoui et al. 2006). In addition to these temperature dynamics studies, many authors have used ^{1}H TD-NMR spectroscopy to analyze the mobility of water and biopolymers at ambient temperature in wheat starch-based systems, including bread crumb samples. The aim was to investigate the evolution of starch structure (i) under cooling, freezing, hydrolysis, pressure, or chemical treatments (Tang et al. 2000, 2001; Hills et al. 2005; Choi and Kerr 2003a, 2004) and (ii) under the influence of various levels of water content (Le Botlan et al. 1998; Tananuwong and Reid 2004; Choi and Kerr 2003b; Rugraff et al. 1996) and of various botanical origins of starch (iii) in the presence of various components or ingredients (Chiotelli et al. 2002; Luyts et al. 2013; Le Grand et al. 2007; Doona and Baik 2007; Roudaut et al. 2009; Wang et al. 2004) and (iv) resulting from the baking process (Bosmans et al. 2012, 2013, 2014; Curti et al. 2011, 2014; Doona and Baik 2007; Engelsen et al. 2001). The processes of both starch swelling and gelatinization were superimposed under these conditions.

The work of Tang et al. (2000) is the reference for NMR measurements of starch-based samples to date, but by cooling the samples. They carried out ^{1}H and ^{2}H NMR experiments on simple models based on water-saturated packed bed potato starch samples, in order to interpret the relaxation times measured on starchy products. At 4 °C, four proton fractions were distinguished by their different mobility using a free induction decay (FID) experiment and the Carr–Purcell–Meiboom–Gill (CPMG) spin–echo pulse sequence. Two short components were found on FID at 20 and 80 μs and assigned to starch CH protons and residual water protons, respectively. The two longer T_2 components determined on the CPMG at 1 and 8 ms were assigned to water located in amorphous growth rings and semicrystalline lamellae. In a related study, instead of cooling samples, Tang et al. (2001) confirmed their assignment by heating the same samples up to 90 °C and by using another starch, i.e., waxy maize starch, in heavy (D_2O) or normal water (H_2O) (Tang et al. 2001). They determined (in D_2O at 34 °C) two relaxation times on the FID signal, the first at 10 μs and the second at 500–700 μs. The exact value of this last component is not convincing since a T_2 relaxation time of 1 ms was observed in CPMG for the same component. Measurements performed at the same temperatures in water allowed the assignment of two components to water inside the starch granules at 1 and 5 ms. The two intra-granular water fractions in potato starch were believed to originate from water in slow diffusional exchange with the outside water, the first in the amorphous rings of granules and the second in the amorphous regions within the semicrystalline lamellae of granules (Tang et al. 2000). In addition, a fifth component at 50 ms has been observed using the CPMG sequence and explained as extra-granular water in a heterogeneous environment within zones more or less rich in water or amylose and showing fast chemical exchanges with starch protons at the granule surface or due to amylose leaching. Finally, it must be pointed out that most studies based their interpretations on the T_2 value without analyzing the evolution of their relative intensity, except those demonstrating that a careful analysis of both relative intensities and T_2 relaxation times improves the interpretation of the NMR results and expands the potential of NMR for quantitative analysis (Assifaoui et al. 2006; Le Grand et al. 2007).

The main aim of the study presented here was to understand and interpret the NMR signal measured on wheat starch-based complex systems such as dough for bread making. The strategy was therefore to perform TD-NMR measurements upon heating (20–90 °C) on wheat starch-based model systems with water content close to that of dough used to obtain a dense loaf of bread (45 % of the total wet weight). The systems studied consisted of wheat starch, starch, and gluten or wheat flour, and yeast with or without added salt. In contrast to all previous studies, the NMR data were acquired and processed from the combined FID-CPMG sequence with the aim of determining more accurately fast relaxing T_2 components in the microsecond time range. Previous separation of FID and CPMG sequences did not allow accurate interpretation of the changes in intensity of each T_2 component in terms of structural changes or proton exchanges between each proton fraction. This is the reason why they were barely discussed. A more thorough analysis is challenging since the intensity of each component (proton fraction) can be directly related to its amounts of water and starch protons. The results were compared to the most relevant NMR data reported in the literature, namely the reference work of Tang et al. (2000, 2001), those obtained upon heating non-wheat starch water mixtures (Ritota et al. 2008; Tananuwong and Reid 2004), and those obtained with the model systems and the wheat flour dough before and immediately after cooling (Bosmans et al. 2012).

Materials

Native wheat starch (11.4±0.1 % moisture), named starch powder (SP), was provided by Merck Millipore (Guyancourt, France). Wheat flour (13.61±0.25 % moisture, 9.24±0.43 % protein, 0.42±0.05 % ash, 73.14±1.08 % starch, 1.72±0.06 % total sugar, 0.97±0.09 % fat, 0.90 % total dietary fiber, 23.7±1.68 % wet gluten) and native gluten (8.14±0.15 % moisture, 80.56±1.63 % protein, 2 g/g water binding capacity) were obtained from Fidelinka Milling Company (Beograd, Serbia). The commercial quality of wheat flour was defined by farinograph water absorption with

a softening degree of 65 BU, alveograph deformation energy of 144×10^{-4} J, and amylograph peak viscosity of 1230 BU.

For salted samples, sodium chloride was dissolved in distilled water in order to obtain a solution containing 2 % salt (compared to the starch or flour wet weight) which was then mixed with starch, the starch–gluten mixture or the flour (used for dough). The water content for the model samples was adjusted with distilled water to 44.7 % of the total sample wet weight. The model samples were blended manually to a homogeneous mixture, while the dough, prepared with fresh yeast (2.5 % of the flour wet weight), was mixed in a kneader for 17 min.

The water content of each sample was determined by the following: The humid samples were weighed before being dried in an oven at 103 °C for 24 h, then the remaining dry matter was weighed to calculate the evaporated water content, determined as 44.9±0.4 % for dough and 44.7 %±0.5 % for model samples (Table 1).

NMR tubes were filled to about 10 mm in height for model systems, and up to 5 mm for dough because of the occurrence of the fermentation process. All the tubes were hermetically closed and weighed, before being placed in the homogeneous region of the NMR magnet. A Teflon rod was introduced into the tube to maintain the optic fiber (Neoptix Inc., Canada) for online temperature measurement and to reduce the vertical expansion of dough and the evaporation of water. Each sample was prepared in triplicate (18 samples in total), and the final results were expressed as a mean value with the associated standard error.

Table 1 shows the detailed composition of five samples analyzed (for a final weight of 50 g for model systems and a total of 2500 g of flour in dough recipes), and their starch/water ratio and total water content.

Methods

^{1}H NMR measurements were performed using a time-domain spectrometer (Minispec BRUKER, Wissembourg, Germany) operating at a resonance frequency of 20 MHz. The NMR system was equipped with a temperature control device connected to a calibrated optic fiber (Neoptix Inc., Canada) allowing for ±0.1 °C temperature regulation. The spin–spin relaxation times (T_2) were measured from the simultaneously recorded free induction decay (FID) and Carr–Purcell–Meiboom–Gill (CPMG) pulse (Meiboom and Gill 1958) curves. The sampling rate for the acquisition of the FID was one point per 0.4 μs, and the delay between the 90° and 180° pulses of the CPMG sequence was 0.1 ms. A total number of eight scans were recorded with a recycle delay of 2 s. Measurements were performed at each 10 °C step between 20 and 90 °C. Before signal acquisition, 15 min was allowed so that the equilibrium temperature could be reached.

Determination of the relaxation time and the associated relative intensity is known to be sensitive to the fitting method selected. To exclude maladjustment, we compared the CPMG results obtained with two different methods: Marquardt's discrete method (Marquardt 1979) and the continuous maximum entropy method (MEM) (Mariette et al. 1998). The same relaxation times were found for both methods. We therefore decided to use the Marquardt method because the MEM method used is not yet available for analyzing Gaussian decay curves.

The NMR signal of the starch powder was fitted using the combination of a sinc function and Gaussian broadening in addition to an exponential function (Eq. 1), while for model systems and dough, two Gaussian curves and the sum of two or three exponentials (n=2 or 3) were used (Eq. 2):

$$I(t) = I_1\exp\left(-t/T_{2(1)}\right)^2\frac{\sin bt}{bt} + I_2\exp\left(-t/T_{2\,(2)}\right) + offset \qquad (1)$$

$$I(t) = \sum_{i=2} I_i\exp\left(-t/T_{2\,(i)}\right)^2 + \sum_{j=1}^{2or\,3} I_j\,\exp\left(-t/T_{2\,(j)}\right) + offset \qquad (2)$$

where $I(t)$ is the intensity of the total relaxation signal, t is the time of the relaxation process, b is a constant, $T_{2\,[i/j]}$ is the spin–spin relaxation time of component i or j, and $I_{i/j}$ is the associated signal intensity. i and j refer to any of the relaxing components of FID and CPMG, respectively.

Table 1 Averages and standard deviations of water content (%), starch/water ratio, and wet weight (gram) of constituents used to prepare model systems and dough

Recipe	Starch	Gluten	Flour	Yeast	Salt	Starch/water ratio	Water content (%)
SW	30.6					1.2	45.3±0.2
SWS	30.4				0.6	1.2	44.4±0.2
GSWS	27.7	2.8			0.6	1.1	44.4±0.1
DS			2500	65.5	50	1	44.5±0.2
D			2500	62.5		1	45.3±0.2

SW starch–water, *SWS* starch–water–salt, *GSWS* gluten–starch–water–salt, *DS* dough with salt, *D* dough without salt

To study the component intensities in the different systems quantitatively, the concept of mass intensity is introduced below. The contribution of $S(i)$ (in volts) to the total NMR signal of a component i of mass m_i can be expressed as mass intensity (MI_i) (in volts per gram):

$$MI_i = \frac{S(i)}{m_i} \quad (3)$$

Because $S(i)$ is directly dependent on the receiver gain, all MIs expressed in this study have been converted to a constant receiver gain (75 dB).

Curie's law provides a linear relationship between the mass intensity of a pure constituent MI_i (V/g) and the inverse of temperature (in kelvin). This straight line can be simulated for water if its NMR signal intensity S_i at 20 °C and 75 dB and the line slope for pure water measured in the same conditions are known.

One-way ANOVA test was carried out using the software Statgraphics (Centurion) to detect significant differences (95 % degree of confidence) between the NMR parameters (T_2 values and associated signal amplitudes) of different model samples. F-ratio was calculated as an indicator of whether, based on the variability within each group, the means were significantly different. The Fisher's least significant difference (LSD) test was used to detect significant differences between sample models.

Results

T_2 NMR relaxation times were measured under the same conditions for six starchy samples: wheat starch powder (SP), a starch–water mixture with (SWS) and without salt (SW), a starch–gluten–water mixture with salt (GSWS), and two dough recipes based on wheat flour and yeast containing the same total water content with or without added salt (DS and D, respectively).

Two T_2 components were found for SP, the first with a T_2 value of 26 μs and a relative intensity close to 81 % and the second with a T_2 of 592 μs representing 19 % of the total signal (Table 2). The ANOVA calculations indicated strong discrimination in this sample compared to the others due to its low water content. The high value of the F factor for $T_2(2)$ was governed by SP that displayed a $T_2(2)$ value that was statistically different compared to the other hydrated samples.

Given the mass intensity of pure water, which is 18.96 V/g for a receiver gain of 75 dB at 20 °C and the amount of water in the SP sample (27.3±2.9 mg), the expected signal intensity was 0.52±0.05 V. This value is close to the intensity of 0.58 V measured for the second component of SP, confirming that this component, at 592 μs, could be assigned to water protons. The same approach was used for the first component, assuming that the proton density (PD) of starch powder was equal to the proton density of glucose. The mass intensity of starch was calculated from Eq. 4:

$$MI_{starch} = \frac{1}{I_{tot}} * \frac{PD_{water}}{PD_{glucose}} * MI_{water} \quad (4)$$

with I_{tot} corresponding to the total intensity of the NMR signal in SP (see Table 2), $PD_{water}=2/18=0.111$, and $PD_{glucose}=12/180=0.067$.

The expected signal intensity of starch was calculated from the mass intensity of starch $MI_{starch}=10.44$ V/g and the starch content (dry weight) in SP (211.2±22.1 mg). The calculated intensity of the first component was 2.21±0.23 V compared to the measured intensity of 2.44 V. The first T_2 component in SP could therefore be assigned to the relaxation time of the CH protons from starch.

After the addition of water to the starch powder sample (SW), four T_2 components could be measured at 20 °C (for a final water content of 45.3±0.2 %): two T_2 relaxation times at 18.4±0.2 and 52.8±1.8 μs and two longer times at 2.45±0.05 and 17.38±1.36 ms, as shown in Table 2. The relative intensity of the first and second components, $A(1)$ and $A(2)$, decreased from 80.7 to 31.9 % and from 19.3 to 7.0 %, respectively, while new components appeared, characterized by relative intensities of 21.7 and 39.4 % for $T_2(3)$ and $T_2(4)$, respectively. Based on the total mass of SW (466.6±20.2 mg) and its water content (45.3±0.2 %), the expected signal intensity for water should have been 4.00±0.17 V, thus corresponding to 61 % of the total NMR signal of SW. This relative signal intensity corresponded to the addition of the relative intensities $A(3)$ and $A(4)$.

Addition of salt (2 % w/w) to the starch–water mixture (SWS) had no influence on T_2 values or relative intensities compared to SW (Table 2). Based on ANOVA calculations, the parameters measured for SW and SWS were not statistically different, except the $T_2(3)$, but with a low F factor (difference hardly significant). The discrimination displayed for $A(1)$ was not supported by the standard deviations. When gluten was added (GSWS) to the salted starch–water mixture (for a final content of 5.6 % of the total wet weight), the NMR signal could also be decomposed into four T_2 values at 18.7±0.1 μs (1), 41.6±15.4 μs (2), 2.20±0.03 ms (3) and 18.15±0.22 ms (4) (Table 2). Doubling was observed for $A(2)$ and a slight decrease for $A(1)$ in the GSWS sample compared to SWS. These significant differences were clearly demonstrated by the LSD tests, showing a net discrimination of these parameters for GSWS (groups indicated by d for $A(1)$ and c for $A(2)$ in Table 2). The signal loss (decreasing in $A(1)$) could be explained by the lower starch/water ratio in GSWS to keep the water content constant in each sample (Table 1). The high additional relative intensity of the second component was consistent with an additional proton fraction from the gluten

Table 2 Averages and standard deviations for T_2 values (ms), associated relative intensities A (%), total signal intensity (volt), and total wet mass (gram) for SW, SWS, and GSWS model systems and for salt ed and unsalted dough DS and D at 20 °C

	$T_2(1)$	HG	$A(1)$	HG	$T_2(2)$	HG	$A(2)$	HG	$T_2(3)$	HG	$A(3)$	HG	$T_2(4)$	HG	$A(4)$	HG	$T_2(5)$	$A(5)$	I_{tot}	m_{tot}
SP	0.0261	a	80.67	a	0.5921	a	19.33	a											3.02	0.260
	±0.0002		±0.76		±0.0018		±0.99												±0.15	±0.021
SW	0.0184	b	31.92	b	0.0528	b	6.97	b	2.45	b	21.70	b	17.38	b	39.41	b			6.60	0.467
	±0.0002		±0.64		±0.0018		±0.90		±0.05		±0.35		±1.36		±0.33				±0.21	±0.020
SWS	0.0183	b	31.83	bc	0.0458	b	6.43	b	2.20	bc	21.82	b	18.31	b	39.91	b			6.99	0.502
	±0.0002		±0.65		±0.0023		±0.90		±0.05		±0.24		±0.24		±0.16				±0.30	±0.022
GSWS	0.0187	b	26.63	d	0.0416	b	12.94	c	2.20	bc	21.27	b	18.15	b	39.17	b			7.30	0.502
	±0.0001		±2.14		±0.0154		±1.88		±0.03		±0.24		±0.22		±1.26				±0.14	±0.003
DS	0.0187	b	30.24	bc	0.0583	b	5.52	b	1.80	cd	13.11	c	8.57	c	18.79	c	23.08	32.34	3.73	0.263
	±0.0007		±0.76		±0.0022		±0.78		±0.03		±0.60		±0.6		±1.17		±0.79	±0.54	±0.33	±0.022
D	0.0186	b	29.98	c	0.0576	b	5.89	b	1.98	d	14.53	d	9.67	c	25.00	d	25.37	24.61	3.35	0.2
	±0.0007		±0.34		±0.0104		±0.84		±0.16		±0.93		±0.91		±3.56		±2.08	±4.59	±0.15	±0.013
F factor	84.30		945.88		1380.83		99.67		10.51		95.97		82.86		37.24					

The F factor was provided by the ANOVA test. Letters (a to d) used in HG columns (homogeneous group) indicate belonging to the same homogeneous group with a 95 % degree of confidence (LSD test)

with the $T_2(2)$ value at 41.6±15.4 μs. As the mass density (proton mass over the total molecular mass) of gluten, starch, and water was different, a direct relationship between the mass intensity of (2) and the relative mass of each constituent was not possible.

Comparison between the DS and D dough samples (using wheat flour and yeast) and the model recipes indicated an additional $T_2(5)$ component at 23.08±0.79 and 25.37± 2.08 ms, respectively, which represented 23–25 % of the total signal intensity and, when added to (3) and (4) components, resulted in 64.19±0.07 % of the total signal, thus slightly higher than the expected signal for water (61 %, see above). Compared to model samples, the dough samples displayed significantly different mean values of $T_2(3)$, $A(3)$, $T_2(4)$, and $A(4)$ and could be discriminated statistically from the other homogeneous groups with fairly high F values (Table 2).

Compared to the DS sample, the unsalted dough D displayed similar T_2 values at 18.6±0.7 μs, 57.6±10.4 μs, 1.98±0.16 ms, 9.67±0.91 ms, and 25.37±2.08 ms. However, the relative intensity of (5) was lower in D in favor of (4) in DS at 20 °C as confirmed by the LSD test which discriminated $A(4)$ of DS from $A(4)$ measured for D (Table 2, groups c and d, respectively). Slightly lower T_2 values were observed for the third component (3) for both DS and D dough compared to the model systems (1.8 ms compared to 2.2 ms), and the difference was significant for the fourth component (4), which was half that for dough (9 ms instead of 18 ms).

NMR measurements of T_2, while the temperature was increased in 10 °C steps between 20 and 90 °C, indicated some T_2 changes and mass intensity variations between the different proton fractions. Based on the assignment described above for $T_2(1)$ and $T_2(2)$ measured on the wheat starch powder sample (SP), the mass intensity of each T_2 component could have been calculated using either the starch mass or the water mass in the sample. The evolution of the mass intensity calculated for the two first components is presented as a function of the inverse of temperature (K) in Fig. 1 for SP and SW samples. For SP, the mass intensities of the starch (1) and water signals (2) obeyed Curie's law and thus decreased, whereas the temperature was increased due to the magnetic susceptibility dependence on temperature. The slope of the straight line for the water signal in SP (5594 V/K) was very similar to that of pure water (5579 v/K) measured in the same conditions (75 dB, 20 °C). In the starch–water mixture (SW), the NMR signal for the water phase could be explained by the third and fourth components (see above) detected in the CPMG signal. Thus, the two short relaxation times $T_2(1)$ and $T_2(2)$ of FID were characteristic of starch protons. This is why their mass intensities were calculated on the basis of the starch content in SW. In this sample, a significant decrease in the mass intensity of (1) could be detected upon heating, whereas for the second starch component (2), the mass intensity increased between 20 and 50 °C and then decreased

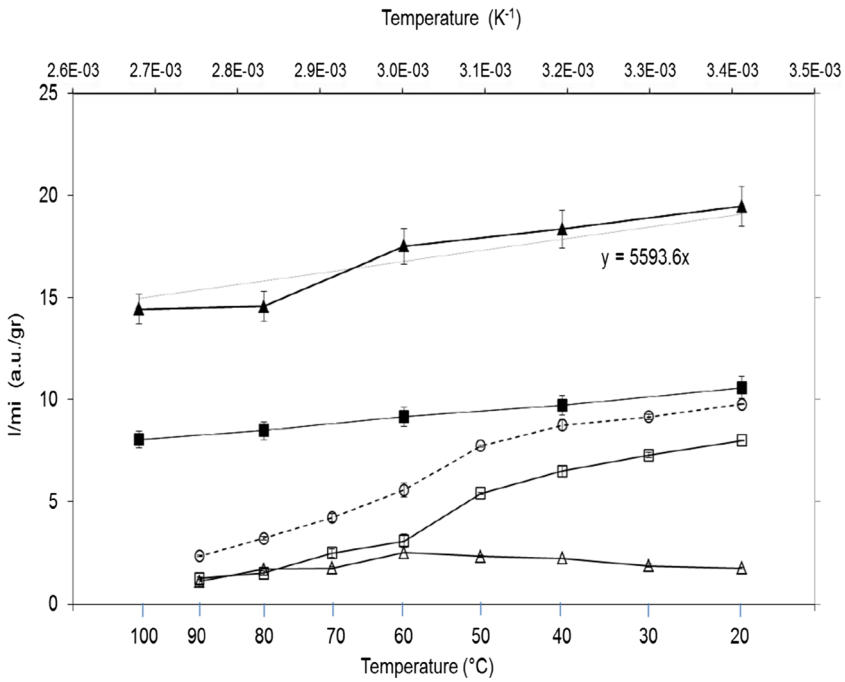

Fig. 1 T_2 mass intensity of components (1) and (2) as a function of inverse of temperature (squares and triangles, respectively) determined on the wheat starch powder sample (SP—*filled symbols*) and the starch–water sample (SW—*empty symbols*). *Dotted line* and *circles* represent the mass intensity of (1+2) in SW. I/m_i is the mass intensity calculated on the basis of either the water mass or the starch mass in the sample

according to Curie's law. Addition of the mass intensities from (1) and (2) gave the curve symbolized by circles. For temperatures between 20 and 40 °C, this curve was very close to Curie's line determined for (1) in SP and indicated that the loss of the mass intensity of (1) was compensated for by the increase in (2) at low temperatures. The slight underestimation of the signal intensity of starch (1+2) in SW compared to SP can be explained by the loss of some starch protons or by an effect of the fitting models used for the determination of the relaxation time.

However, (1)+(2) mass intensities decreased above 40 °C, and more significantly compared to the expected decrease due to Curie's law. Thus, above 40 °C, a large fraction of the starch protons contributed to the CPMG signal characterized by higher relaxation times.

The same investigations were performed for CPMG components measured for the SW sample (Fig. 2). An additional T_2 component (5) was measured at 50 °C, corresponding to the splitting of the fourth component (4) into two water fractions. In this case, the mass intensities of components (3), (4), and (5) were calculated on the basis of the water mass in the sample, and their addition was compared to Curie's straight line simulated for pure water (dotted line and crosses in Fig. 2). As shown in Fig. 2, the total signal measured (3+4+5) for water protons obeyed Curie's law up to 40 °C but was overestimated compared to the signal deduced from the water content of the SW sample. This signal excess between 20 and 40 °C corresponded to the signal missing in Fig. 1 and confirmed a contribution of starch-exchangeable protons to the CPMG signal, whereas starch granules swelled. By increasing the temperature to 40 °C, the total water signal in SW (filled squares) increased to the same level as the FID signal from starch decreased (circles in Fig. 1). Thus, the contribution of starch protons to the water signal increased strongly above 40 °C. Moreover, in this temperature range, component (4) was mainly constant while (3) decreased, with a slope very similar to that of the pure water. At 50 °C, the novel T_2 component (5) appeared and increased with temperature, while strong variation in the distribution between the three components was observed (Fig. 2).

Figure 3 shows the variations in relative intensity and T_2 values against temperature (expressed in Celsius for purposes of clarity) for each component from (1) to (5). For each sample, the trends of the T_2 relative intensity and values were very close, especially when SW, SWS, and GSWS model systems were compared.

Regardless of the sample (model or dough, salted or unsalted), the T_2 values of (1) and (2) components hardly changed between 20 and 60 °C and slightly increased with temperature above 60 °C (Arrhenius effect) but significantly increased for unsalted dough D. For each sample, the relative intensity of (1) showed a continuous decrease over the temperature range, while the relative intensity of (2) increased slightly with temperature up to 60 °C and then decreased. The relative intensity loss of (1) was more pronounced than the signal decrease due to Curie's law, as explained and shown above for SW (Fig. 1). Indeed, if we assumed a signal decrease only explained by Curie's law, then the expected value for the relative intensity of (1) at 90 °C would have been 23 %, which is high compared to

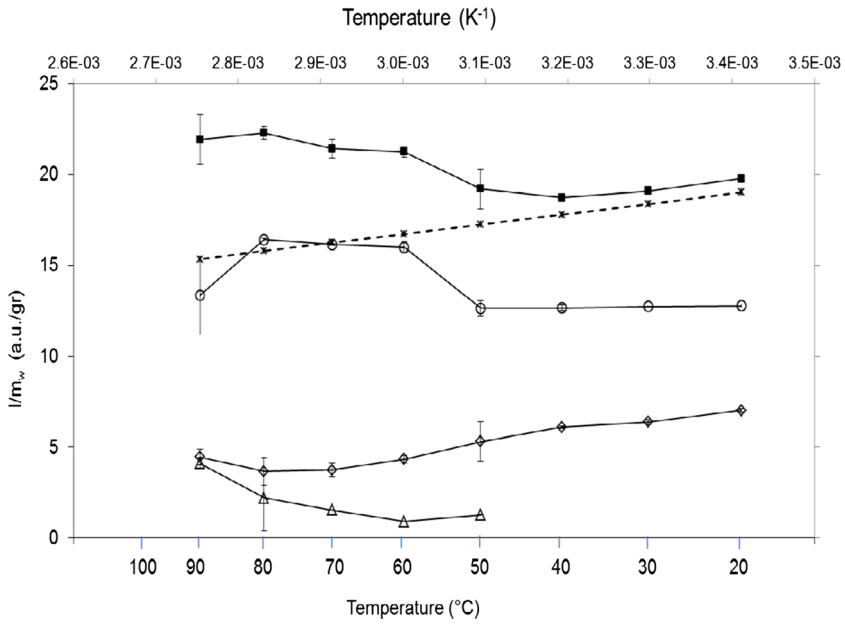

Fig. 2 T_2 mass intensity of components (3) to (5) as a function of inverse of temperature for the starch–water sample (SW) (*empty diamonds* for (3), *empty circles* for (4), *empty triangle* for (5), and *filled squares* for (3+4+5)). The *straight dotted line* represents the intensity evolution for pure water. I/m_w is the mass intensity calculated on the basis of the water mass

the experimental values that were between 5 and 12 %, depending on the sample (Fig. 3).

The relative intensity of (3) decreased slightly on model systems, whereas (4) remained constant below 50 °C. For dough, the relative intensity of (3) was mainly constant as for (4+5) since (4) increased by the same amount that (5) decreased. The T_2 values of (3) were comparable and fairly constant for dough and model systems in this temperature range, while T_2 values for (4) changed inversely with temperature (increased for dough, decreased for model systems). On the other hand, both the relative intensity and the T_2 values of (3) and (4) continued to be lower for dough than for the model systems. Above 50 °C, changes observed in (3) differed from one sample to another, with the same trend for model systems and for dough (DS and D). The relative intensity and T_2 value of (3) for model systems changed in the opposite manner to dough, since in the model systems, both decreased with temperature, whereas in dough, they increased.

The evolution of the T_2 value of components (4) and (5) was more complex. In accordance with Arrhenius law, an increase in the T_2(4) values was detected for each sample above 70 °C. Compared to salted model systems, these changes were weaker for the SW sample. Component (5) appeared only at 50 °C for SW, SWS, and GSWS samples, with a slightly lower T_2 value for the SW unsalted model but with the same increase with temperature. D and DS dough displayed the same T_2 values for both components (4) and (5) and a slight increase up to 60 °C, but above this temperature, the increase in T_2 was significantly higher for the unsalted D sample compared to the DS sample.

Discussion

Assignment of T_2 Distributions at 20 °C

For years, several studies have been performed on different starch types (rice, wheat, etc.), at levels of water content varying between 41 and 78 % and sometimes on water-saturated packed beds of starch, without specifying the real water content. The NMR results for each of these were interpreted on the basis of the assignment proposed by Tang et al. (2000, 2001).

At a level of water content very close to ours and using the same equipment, Bosmans et al. (2012) found five T_2 components for a wheat starch–water sample without salt at 25 °C. In FID experiments, two T_2 components were determined relaxing at 20 μs (A) and 80 μs (B). Three others were found at 500 μs (B′), 3 ms (C), and 10 ms (D) by performing a CPMG experiment. Based on the results of Tang et al. (2000, 2001), Bosmans et al. (2012) proposed that the (B) and (B′) values corresponded to the same proton fractions. The T_2 values determined in our study for wheat starch hydrated at 45.3±0.2 % were studied at 20 °C and were found to be close to these results: 18.4±0.2 μs (1), 52.8±1.8 μs (2), 2.45±0.05 ms (3), and 17.38±1.36 ms (4) (see Table 2). Our data were acquired using a combined FID-CPMG sequence which was more convenient to compare the mass intensities of all T_2 components. In addition, our results confirmed that only four T_2 components described the various proton fractions of the starch–water mixture at 20 °C. This was confirmed by comparing the results obtained from two different processing approaches, one using a continuous fitting method and the other using a discrete fitting method (see "Materials" and "Methods").

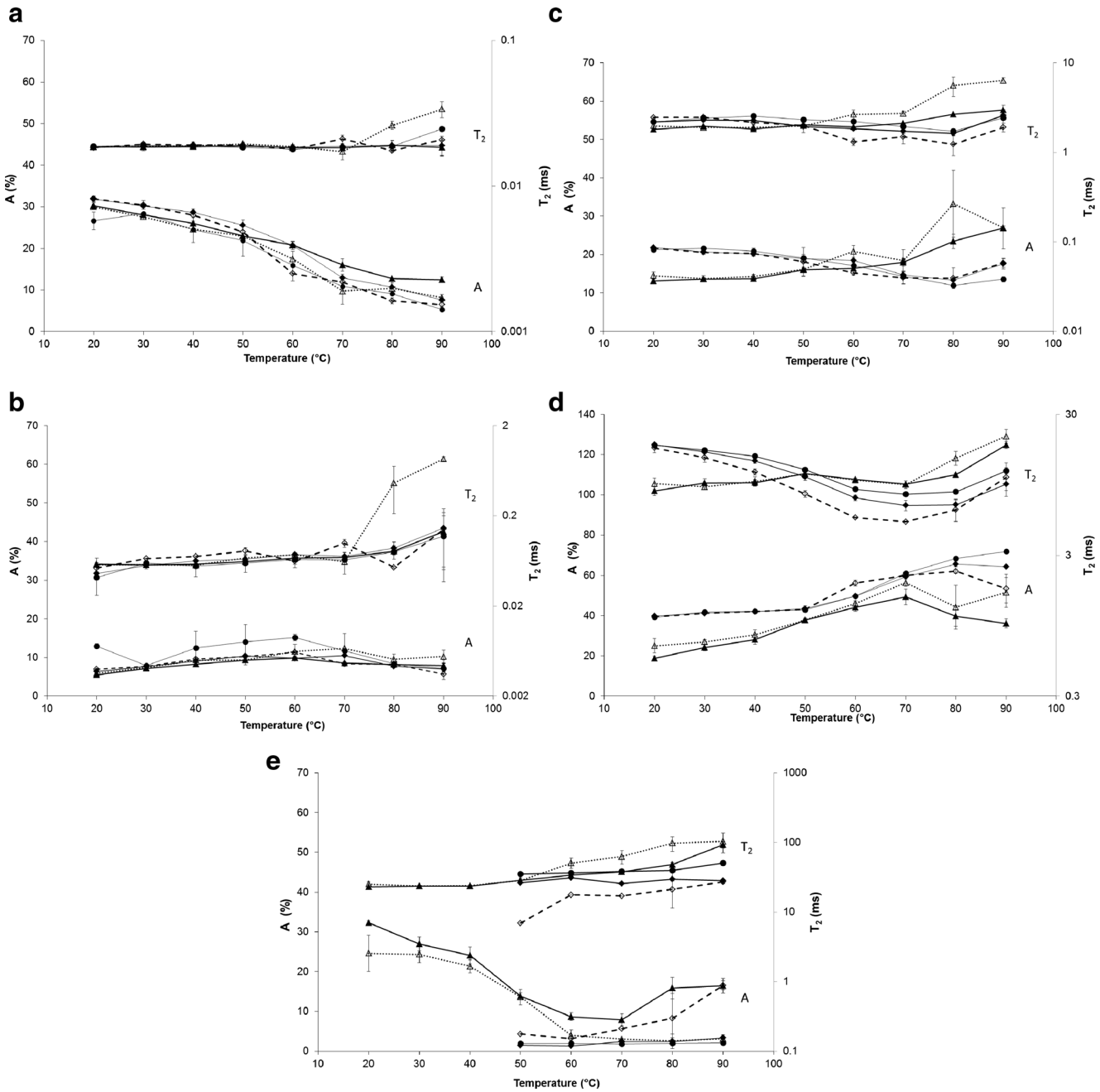

Fig. 3 Variations in the relative intensity and values (logarithmic scale) of T_2 components (1) to (5) (**a**–**e**) for SW (*empty diamonds*), SWS (*filled diamonds*), GSWS (*filled circles*), DS (*filled triangles*), and D (*empty triangles*) samples as a function of temperature (°C). **d** displays a larger ordinate scale for amplitudes A in order to show more clearly the T_2 variations in the same figure

In order to assign these T_2 values to specific proton populations precisely, Bosmans et al. (2012) compared results from wheat starch to those from maize starch, waxy starch, and high amylose (66 %) starch samples. On the basis of the previous assignment proposed by Tang et al. (2000, 2001), they concluded that the (A) component corresponded to nonexchangeable CH of amylopectin in crystalline regions of granules, (B and B′) to nonexchangeable CH of starch in amorphous regions of granules, (C) to water in exchange with hydroxylated groups of starch in intra-granular spaces, and (D) to water in exchange with hydroxylated group of amylose in extra-granular spaces (Bosmans et al. 2012). However, they did not explain why the high amylose starch sample displayed the (A) component, with T_2 value and intensity similar to the waxy sample (rich in amylopectin), or why the (B) component, which was believed to represent protons from amylose, was absent from both of these samples. This result will be discussed by analyzing the thermal progress of these T_2 components.

The hypothesis that the (D) component corresponded to extra-granular water, with a short T_2 value compared to that of bulk water, was supported by the fact that this water fraction contained amylose at ambient temperature. This assignment was supported by Chiotelli et al. (2002) who proposed that leaching of amylose can occur slowly from the granules into the extra-granular water at room temperature. The fourth component (4) measured in our samples was also characterized by a short T_2 relaxation time (9–18 ms). At 20 °C, the mass intensity MI(4) measured on SW was lower than for pure water, and on heating, it remained constant instead of decreasing due to Curie's law (see below). Addition of the mass intensity of (3) and (4) revealed a higher value than that of pure water at the expense of (1)+(2). This result supports the hypothesis that amylose leaching can occur at ambient temperature.

The second model system investigated in the present study was the wheat starch–water sample containing 2 % (*w*/*w*) salt (NaCl). Addition of salt to food samples is a common practice, especially in cereal-based foods such as bread, biscuits, and breakfast cereals. Its role is to enhance flavor perception, but it can also act on the dough-handling properties, the yeast activity, and the transformation of starch during the processing of starchy food (Miller and Hoseney 2008; Uthayakumaran et al. 2011). Chiotelli et al. (2002) showed that the addition of salt delayed the gelatinization process at higher or lower temperatures, depending on salt concentrations ranging from 0 to 16 % (of the total wet weight). Unfortunately, they performed NMR measurements only for salt and water concentrations of 7 and 60 %, respectively, or higher. In their study, performed at 25 °C, the T_2 value assigned to extra-granular water was found to increase slightly with the salt concentration (from 32 ms at 0 % to 41 ms at 7 % NaCl), whereas few changes were observed for the other components. These results, combined with those obtained by differential scanning calorimetry (DSC) and other techniques, were interpreted in terms of the "structure-breaking"-like effect of salt which reduced the starch–water interactions (Chiotelli et al. 2002). In our study, with a lower salt concentration and a higher starch content than in the study of Chiotelli et al. (2002), the SWS salted model system gave exactly the same T_2 distributions as the SW sample at 20 °C (Table 2).

No influence was observed following the addition of gluten to the salted starch–water sample (at 20 °C) except for higher relative intensity of the second component (2) which increased twofold. The ANOVA tests confirmed this significant difference compared to SW and SWS samples. Component (2) was found in the GSWS model at 41.6±15.4 μs. It was characteristic of nonexchangeable protons of amorphous starch (amylose), but its net increase by the addition of gluten suggested that (2) also contained some protons from gluten chains with low mobility and low contact with water. This assignment had also been proposed by Bosmans et al. (2012) who, in addition, suggested that the first short T_2 component might contain populations corresponding to nonexchangeable CH of gluten chains without contact with water. This hypothesis was based on the "sheet" model structure proposed by Kontogiorgos (2011) and was supported by T_2 measurements on gluten–water and gluten-deuterated water samples (Bosmans et al. 2012; Doona and Baik 2007; Wang et al. 2004). However, in our GSWS sample containing gluten, no increase in (1) was observed. There was instead a slight decrease due to a lower starch/water ratio (Table 1), suggesting that in our case, the nonexchangeable CH of gluten chains was more mobile and provided a single T_2 population (2) with a slight disturbance of the starch proton fraction characterized by the short T_2 at 18.7 μs (1). We emphasize that our recipe contained salt which could shield the charges on the gluten proteins, allowing them to associate differently. Addition of salt in gluten–water suspensions (monolayer films of gluten) or in breadmaking has been shown to improve inter-polymer interactions and to reduce water–polymer interactions, thus influencing the mobility of each constituent, especially the gluten (Balla et al. 1998; Hoseney 1994).

The competitive water–starch and water–gluten interactions should affect the T_2 distributions for water in exchange with labile protons (in OH, NH, SH functional groups) from starch and gluten (Wang et al. 2004). These water proton populations should correspond to the third component (3) at around 2 ms and that at 18 ms (4) (intra-granular and extra-granular water fractions, respectively, in starch–water mixtures). We found that the addition of gluten had no effect on the (3) and (4) T_2 values and intensities measured at 20 °C, supporting the hypothesis that the water absorption by starch was hardly modified in the presence of gluten (5.6 % of the total weight), as proposed by other authors (Doona and Baik 2007; Wang et al. 2004). Instead, without influencing the mobility of molecules (same T_2 values for each component), the relative intensity of (2) was considerably increased due to additional protons from gluten sheets. This result was confirmed by the ANOVA calculations on $A(2)$ that were significantly different for GSWS compared to the other samples.

Comparison of the T_2 relaxation times and intensities measured at 20 °C between the GSWS model recipe and DS salted dough (using flour and yeast) indicated (i) very similar values for (1) and (2) components, (ii) slightly lower values and intensities in DS dough for (3) and (4), and (iii) the appearance of a new extra-granular water fraction (5) in DS dough. Component (5) did not appear consistently in previous studies, and when it did, it did not generate much interest. For potato starch, this component with a longer T_2 value was observed only for partly acid-hydrolyzed starch samples (Tang et al. 2001) and was attributed to the formation of a dilute amylose gel. The appearance of this T_2 component could only be explained by a slow diffusion process between two water compartments. Given its higher T_2 value, we

hypothesized that (5) represented a second fraction of extra-granular water in slow diffusional exchange with the other water fractions due to the structural heterogeneity of the systems. The distribution of the extra-granular water should, moreover, be significantly different in dough due to a different starch/water ratio (close to 1 for GSWS and dough compared to 1.2 in SW and SWS systems, see Table 1) and thus different water sorption capacities. The greater heterogeneity might also be linked to the dough liquor (liquid lamellae), an aqueous phase already described in the literature and thought to maintain the bubble structure in breadmaking (MacRitchie 1976). The lower T_2 values observed for (3) and particularly for (4), as confirmed by the ANOVA tests, could be interpreted in terms of less available water and thus stronger water–biopolymer interactions inside and outside the starch granules or the gluten sheets in dough. The lower intensities were compensated for by the additional component (5). It should be noted that the wheat starch used in model systems was not extracted from the flour used to prepare dough but was a commercial product (see experimental section) and might, therefore, have differed in terms of water distribution.

When dough was prepared without salt (D recipe), the T_2 values were very similar to those of the salted recipe (DS), but the relative intensity of (5) was weaker because of the greater intensity of (4), confirming that at an ambient temperature, the addition of salt had a minimal influence on T_2 measurements and only affected extra-granular distribution.

Reversible Swelling-Associated Changes in T_2

Variations in the T_2 values and intensities of the various samples upon heating demonstrated that the temperature increase induced proton transfers between components (1) and (2) (Fig. 3a, b) and also between them and the three water fractions (3), (4), and (5) (Fig. 3c–e). Before the gelatinization transition, expected to occur at around 50–60 °C, water diffuses into granules and enhances their hydration and swelling. These events are believed to start in more available and less strongly bonded regions, i.e., in the amorphous parts of the starch granules. This water-diffusing fraction is believed to correspond to the intra-granular water phase described in the literature and characterized by a relaxation time T_2 close to 1–2 ms, which corresponds to the third component (3) in the present study. Surprisingly, the mass intensity MI(3) was shown to obey Curie's law between 20 and 50 °C. On the other hand, we observed a slight increase in the relative intensity of (2) concurrent with the relative intensity stagnation of (4) (Fig. 3b, d and in Fig. 1 for SW). A detailed interpretation of these findings is proposed here.

During the reversible swelling process between 20 and 50 °C, the relative intensity decrease of (1+2) with heating could be explained by Curie's law, which deals with the linear dependence of magnetic susceptibility relative to the inverse of temperature. However, in the case of only component (1), the signal loss was considerably more pronounced than that expected according to Curie's law, indicating that another phenomenon was occurring at the same time (Fig. 1). As mentioned above and based on the literature, component (1) has classically been assigned to nonexchangeable CH protons of amylopectin in crystalline regions of granules (Tang et al. 2000, 2001). This fraction was expected to be enriched by the addition of gluten, but in our case, the relative intensity of (1) decreased at 20 °C in GSWS, due to a lower starch/water ratio. The continuous and significant decrease in (1) while the granules swelled revealed that this component represents a proton fraction which is potentially transferable to the other components. Therefore, in addition to protons from amylopectin, component (1) might represent CH protons from well-organized structures such as structured amylose (may be complexed with lipids) or water in very constrained zones, as in the crystalline lattice of amylopectin clusters (Tang et al. 2001). The lipid content in wheat starch does not exceed 2 %, and the melting of starch-lipid crystals should occur at temperatures exceeding 90 °C. The contribution of these crystalline structures should therefore be very weak. On small distance scales corresponding to the macromolecular internal structure of a blocklet of starch granules, water is present in the crystalline lattice of amylopectin clusters and has a structural role by hydrogen bonding with the -OH groups of amylopectin. This water fraction, called "channel water" by Tang et al. (2000), was quantified using small-angle neutron scattering (SANS) experiments for water present in the amorphous lamellae and the amorphous background of waxy maize starch containing 45 % of water. For this sample at 20 °C, the water in the crystalline region represented around 7 % of the total water, 43 % was in the amorphous background regions and 50 % in the amorphous lamellae (Jenkins and Donald 1998). Below the gelatinization temperature, these authors showed that the water uptake by the amorphous background region does not come solely from the extra-granular water but also from the amorphous lamellae and to a lesser extent from the crystalline lamellae. This water fraction is expected to relax with a very short T_2 of a few microseconds. However, no repetition of the SANS experiments confirmed these water density changes measured on waxy starch. In addition, our results based on the analyses of the temperature-associated mass intensity evolution of (1) and (2) in the starch powder (SP) and in the starch–water mixture (SW) confirmed that these components represented protons from starch. As component (1) significantly decreased during the swelling process and was characterized by a very short relaxation time at 18 μs, we propose that it contains CH protons from both crystalline amylopectin and amylose. This interpretation is consistent with the results of Bosmans et al. (2012) who observed a fairly intense short T_2 component at around 18 μs for a high-amylose starch sample (Bosmans et al. 2012).

Moreover, the possibility of co-crystallization between amylose and amylopectin and/or the penetration of amylose into the amorphous regions of the cluster (where the branch points are located) has already been proposed (Jenkins and Donald 1995).

Amylose is known to be present mainly in amorphous channels separating large and small blocklets of the semicrystalline lamellae of granules and in the amorphous growth rings of granules (also called the amorphous background regions) (Gallant et al. 1997; Tang et al. 2000). Because of its insoluble and linear polymer structure, amylose is expected to be characterized by a short relaxation time between 80 and 500 μs. Using a combined FID-CPMG sequence, our analyses confirmed that a single relaxation time was measured in this time range at 42.7±7.3 μs (2). This component in SW at 20 °C represented 18 % of the total signal for starch (FID signal). This is lower than the expected 26–28 % of amylose contained in wheat starch and suggests either a signal lack due to the amylose leaching phenomenon and/or an underestimation due to the amylose contribution in the first component (1) as explained above. The T_2 values of (1) and (2) did not change between 20 and 50 °C, whereas the relative intensity of (2) (Fig. 3b) and its mass intensity (Fig. 1) increased instead of decreasing according to Curie's law. Our results predicted that, in this temperature range, granules swelled by water sorption, as proposed by various authors (Chiotelli et al. 2002; Jenkins and Donald 1998). During this period, the crystalline structure of granules was intact, but our results indicated that the swelling process was accompanied by a CH proton transfer that could be attributed to amylose transfer from crystalline or more constrained structures (1) toward the amorphous parts of granules (2). However, this proton transfer that occurred below 50 °C indicated an overall signal lack, as shown by the FID data compared to the expected starch signal (Fig. 1). This signal lack could be an effect of the fitting models used for determination of the relaxation time. Curiously, it was compensated for by the excess of protons in the water phase and recorded in the CPMG signal (Fig. 2). This phenomenon, that is typical of amylose leaching (Leach et al. 1961), also influenced the T_2 value of the extra-granular water fraction (4) which was characterized by a continuous decrease in model systems, especially for the unsalted starch–water sample (SW).

The relative intensity decrease observed for the intra-granular water fraction (3) between 20 and 50 °C in all the model systems (Fig. 3c) was mainly due to Curie's law as shown on SW (Fig. 2). However, the stagnation of its T_2 value despite higher temperatures indicated greater starch–water interactions because of the swelling process.

For a salt concentration of 7 % in the starch sample hydrated at 60 % (wet starch basis), Chiotelli et al. (2002) proposed that the starch–water and inter-polymer interactions were modified, resulting in higher T_2 relaxation times for water. Recent studies carried out using DSC by Zhu et al. (2009) and by Day et al. (2013) showed that wheat starch granule swelling decreased in the presence of 3 % NaCl in highly hydrated samples (97 % *w*/*w*), particularly when the mixture was heated to 55–65 °C (Zhu et al. 2009). The only effect observed in our case for 2 % salted samples was higher T_2(4) values for salted model systems compared to the unsalted SW sample. This was in accordance with the higher ionic interactions between Na+ and starch granules and hence weaker water–macromolecule interactions in salted samples. Nevertheless, the T_2 relative intensity was neither affected by the addition of salt nor was compensated for by another phenomenon, thus preventing any discussion on the impact of salt on granule swelling.

A redistribution of water was expected to occur between gluten and starch during heating when mixed together. Gluten should release some water, and starch should absorb more water (Eliasson 1983; Wang et al. 2004). The same trend as for the SWS model was observed for water components (3) and (4) when heating the gluten–starch–water mixture (GSWS) below 60 °C, except for T_2(4) values which were higher in the presence of gluten (Fig. 3c, d). Bosmans et al. (2012) showed that, unlike other proteins, heat treatment did not markedly change the proton distribution in the gluten–water sample (Ablett et al. 1988). Although the structure and rheological properties of gluten were changed by heating due to the formation of additional disulfide cross-links and polymerization of gliadins and glutenins, Bosmans et al. (2012) confirmed that these changes did not induce significant changes in NMR T_2 distributions below 50 °C. On the contrary, our results indicated that the addition of gluten in the model systems slightly increased the T_2 relaxation times of the extra-granular water fraction. For dough, both the T_2 values and the relative intensity of the extra-granular water (4) increased with temperature, but due to its splitting into components (4) and (5), evolution of (4) must be discussed with that of (5) (Fig. 3e). For salted and unsalted dough, T_2 values of (4) increased with temperature, while their relative intensity interchanged with the additional "bulk" water (5) component. It seems that this slow diffusional exchange in dough was the predominant effect on the T_2 values of (4) rather than the amylose-leaching process.

Gelatinization-Associated Changes in T_2

The gelatinization of starch granules occurred at temperatures close to 60 and up to 90 °C and then contributed to the crystallinity and organization loss related to starch solubilization and granule disintegration and resulted in the relative intensity decrease of (1) and (2) in favor of the water fractions (3), (4), and (5). A net increase in the T_2 values of (1) and (2) in unsalted dough D was recorded over 70 °C (Fig. 3a, b). This could be linked to thermal activation mechanisms (Arrhenius

effect), but the reason why this effect was significant for unsalted dough D was believed to arise from weaker inter-macromolecule interactions compared to DS, which was expected to be characterized by higher levels of ionic interactions between sodium cations and macromolecules (Chiotelli et al. 2002).

The evolution of the water components (3), (4), and (5) above 60 °C was surprising. This evolution has hardly ever been discussed in previous papers which mainly focused on changes in the starch proton fractions (Fig. 3c–e). For model systems, T_2 values and relative intensities of the intra-granular water fraction (3) decreased in relation to granule disintegration and the expected improvement in viscosity (Donald 2004). The opposite was noted for dough samples. In fact, this component, which was assigned to intra-granular water before gelatinization, had partly disappeared, and over 60 °C probably corresponded to a mixture of intra-granular water and a new water–biopolymer phase, expected to be relatively viscous (Donald 2004), and containing granule fragments, together with molecularly dispersed starch. The evolution of the relative intensity of the intra-granular water phase (3) was rather confusing for model systems over 60 °C, revealing some changes contrary to those observed for dough. However, these changes were concomitant with the appearance of (5) assigned to an additional water–biopolymer fraction. By heating over 60 °C, the extra-granular water components (4) and (5) are believed to contain some granule fragments, which would logically induce an increase in their relative intensity for most samples. The mass intensity of (4) measured on SW over 50 °C was interesting, as it showed an evolution very similar to that of pure water (Fig. 2) and confirmed its assignment to water, which over the gelatinization process has chemical properties close to those of water. The T_2 value of (4) and (5) increased in accordance with Arrhenius law. The U-like evolution of T_2(4) with a minimum close to the gelatinization temperature (60–70 °C) was consistent with previous studies carried out on rice starch–water-saturated samples (Ritota et al. 2008) and starch-based recipes (Assifaoui et al. 2006; Roudaut et al. 2009). The unsalted starch–water model (SW) showed lower T_2 values, regardless of the temperature and a net increase in the relative intensity of T_2 at 60 °C (Fig. 3d). As reported above, studies carried out using DSC (Chiotelli et al. 2002; Day et al. 2013; Zhu et al. 2009) showed that salt shifted the thermal peaks of starch transitions to higher temperatures (from 62 to 70 °C) at water content above 35 % and for 2 % salt content. These changes were interpreted in terms of Na+ ions and starch interactions. The different evolution for (4) observed for the SW sample could indeed support this hypothesis; however, it was not observed in dough.

The unsalted dough (D) displayed higher T_2 values for each component above 60–70 °C than those measured on salted samples. This was not consistent with the structure-breaking-like effect of salt mentioned above. Compared to the relative intensity variations measured for the salted dough (DS), the only noticeable difference was for water component (5) which decreased significantly from 60 °C in the unsalted dough. It seemed probable that the swelling capacity of salted dough DS was reduced over 60 °C compared to the unsalted samples. This is consistent with published findings on the starch granule particle size, which has been shown to be proportional to the starch swelling capacity that decreased in the presence of 3 % NaCl in highly hydrated samples (water content 97 % *w*/*w*), particularly when the mixture was heated to 55–65 °C (Zhu et al. 2009). On the other hand, using DSC, (Leon et al. 2003) detected one endothermic peak at 58 °C for gliadins in gluten samples, whereas two endothermic peaks at 64 and 84 °C were attributed to the glutenin denaturation. Due to the gluten denaturation, the protons of the expelled water fraction should therefore be characterized by greater mobility. It has also been shown in starchy products that peak viscosity is reached at around 80 °C. Above this temperature, more granule ruptures cause a further decrease in viscosity (Donald 2004) which could also explain higher T_2 values for each T_2 component. It can therefore be supposed that, although salt reduces water sorption in dough, the mobility of this extra-granular water fraction can vary due to many phenomena, including gluten denaturation or the overall viscosity changes in heated samples.

Conclusion

Evolution in proton distribution and mobility during heat treatment of wheat starch-based model systems and wheat flour dough revealed that starch swelling and gelatinization were complex processes which influenced the mobility of each constituent and could be studied separately below the starch gelatinization temperature. Various changes in starch were observed: Granules swelled, absorbed water, leached amylose, and lost crystallinity. These events have been investigated in the past using many techniques in attempts to understand the precise structural changes mainly underlying gelatinization. No universally accepted explanation of the swelling and gelatinization processes is available to date. Despite the several time-domain NMR studies, temperature-associated changes have rarely been discussed and, when they were, they involved either the water or the starch proton mobility before and/or after heating but rarely the variations in mass intensity of both with temperature. On the basis of Curie's law, we showed that the investigation of each proton T_2 value and relative or mass intensity change as a function of temperature demonstrated that the shortest T_2 relaxation time (1) was assigned not only to nonexchangeable CH protons from amylopectin but also to those from amylose which

transferred into the proton fraction (2) and enriched the extra-granular water phase (4). This was a direct result of the amylose leaching during the swelling process. Splitting of the extra-granular water phase into two T_2 components, observed in several studies but often not discussed, was attributed to slow diffusional exchange phenomena between different water layers. We also hypothesized that in dough, this water fraction that is present at the ambient temperature might represent the liquid lamellae at the interface of gas bubbles. The impact of salt was also investigated, particularly over 60 °C, a temperature range in which the unsalted dough showed higher T_2 values for each proton fraction, even that assigned to nonexchangeable macromolecule protons. Finally, time-domain NMR spectroscopy was demonstrated to provide not only information on the water and biopolymer mobility but also quantitative data proving that transfer of protons occurs between each proton population with heating, characterized by specific T_2 relaxation times.

Acknowledgments This work was performed using the NMR facilities of the PRISM Research Platform (Rennes, France) which has been awarded an ISO 9001 certification for its activities related to research. The authors thank M. Pojic (FINS, Novi Sad, Serbia) for valuable comments concerning the starch impact on dough structure, as well as G. Collewet (Irstea, Rennes, France) for her help in performing ANOVA calculations.

References

Ablett, S., Barnes, D. J., Davies, A. P., Ingman, S. J., & Patient, D. W. (1988). C-13 and pulse nuclear magnetic-resonance spectroscopy of wheat proteins. *Journal of Cereal Science, 7*(1), 11–20.

Assifaoui, A., Champion, D., Chiotelli, E., & Verel, A. (2006). Characterization of water mobility in biscuit dough using a low-field H-1 NMR technique. *Carbohydrate Polymers, 64*(2), 197–204. doi:10.1016/j.carbpol.2005.11.020.

Balla, A., Razafindralambo, H., Blecker, C., & Paquot, M. (1998). Interfacial properties of gluten monolayers spread on various chloride salt solutions. Effects of electrolytes, salt concentrations, and temperature. *Journal of Agricultural and Food Chemistry, 46*(9), 3535–3539. doi:10.1021/jf971006j.

Biliaderis, C. G. (1992). Structures and phase-transitions of starch in food systems. *Food Technology, 46*(6), 98–109.

Bosmans, G. M., Lagrain, B., Deleu, L. J., Fierens, E., Hills, B. P., & Delcour, J. A. (2012). Assignments of proton populations in dough and bread using NMR relaxometry of starch, gluten, and flour model systems. *Journal of Agricultural and Food Chemistry, 60*(21), 5461–5470. doi:10.1021/jf3008508.

Bosmans, G. M., Lagrain, B., Ooms, N., Fierens, E., & Delcour, J. A. (2013). Biopolymer interactions, water dynamics, and bread crumb firming. *Journal of Agricultural and Food Chemistry, 61*(19), 4646–4654. doi:10.1021/jf4010466.

Bosmans, G. M., Lagrain, B., Ooms, N., Fierens, E., & Delcour, J. A. (2014). Storage of parbaked bread affects shelf life of fully baked end product: a H-1 NMR study. *Food Chemistry, 165*, 149–156. doi:10.1016/j.foodchem.2014.05.056.

Chiotelli, E., Pilosio, G., & Le Meste, M. (2002). Effect of sodium chloride on the gelatinization of starch: a multi measurement study. *Biopolymers, 63*(1), 41–58. doi:10.1002/bip.1061.

Choi, S. G., & Kerr, W. L. (2003a). Effect of chemical modification of wheat starch on molecular mobility as studied by pulsed 1H NMR. *Lebensmittel-Wissenschaft Und-Technologie-Food Science and Technology, 36*, 105–112. doi:10.1094/cchem.2003.80.3.290.

Choi, S. G., & Kerr, W. L. (2003b). H-1 NMR studies of molecular mobility in wheat starch. *Food Research International, 36*(4), 341–348. doi:10.1016/s0963-9969(02)00225-9.

Choi, S. G., & Kerr, W. L. (2004). Swelling characteristics of native and chemically modified wheat starches as a function of heating temperature and time. *Starch-Starke, 56*(5), 181–189. doi:10.1002/star.200300233.

Curti, E., Bubici, S., Carini, E., Baroni, S., & Vittadini, E. (2011). Water molecular dynamics during bread staling by nuclear magnetic resonance. *LWT–Food Science and Technology, 44*(4), 854–859. doi:10.1016/j.lwt.2010.11.021.

Curti, E., Carini, E., Tribuzio, G., & Vittadini, E. (2014). Bread staling: effect of gluten on physico-chemical properties and molecular mobility. *LWT–Food Science and Technology, 59*(1), 418–425. doi:10.1016/j.lwt.2014.04.057.

Day, L., Fayet, C., & Homer, S. (2013). Effect of NaCl on the thermal behaviour of wheat starch in excess and limited water. *Carbohydrate Polymers, 94*(1), 31–37. doi:10.1016/j.carbpol.2012.12.063.

Donald, A. M. (2004). Understanding starch structure and functionality. In A.-C. Eliasson (Ed.), *Starch in food: structure, function and applications (CRC press LLC ed* (pp. 171–199). Cambridge: Woodhead Publishing Limited.

Doona, C. J., & Baik, M. Y. (2007). Molecular mobility in model dough systems studied by time-domain nuclear magnetic resonance spectroscopy. *Journal of Cereal Science, 45*(3), 257–262. doi:10.1016/j.jcs.2006.07.015.

Eliasson, A. C. (1983). Differential scanning calorimetry studies on wheat starch-gluten mixtures. I. Effect of gluten on the gelatinization of wheat starch. *Journal of Cereal Science, 1*, 199–205.

Engelsen, S. B., Jensen, M. K., Pedersen, H. T., Norgaard, L., & Munck, L. (2001). NMR-baking and multivariate prediction of instrumental texture parameters in bread. *Journal of Cereal Science, 33*(1), 59–69. doi:10.1006/jcrs.2000.0343.

Fan, D. M., Ma, S. Y., Wang, L. Y., Zhao, H. F., Zhao, J. X., Zhang, H., et al. (2013). H-1 NMR studies of starch-water interactions during microwave heating. *Carbohydrate Polymers, 97*(2), 406–412. doi:10.1016/j.carbpol.2013.05.021.

Gallant, D. J., Bouchet, B., & Baldwin, P. M. (1997). Microscopy of starch: evidence of a new level of granule organization. *Carbohydrate Polymers, 32*(3–4), 177–191. doi:10.1016/s0144-8617(97)00008-8.

Hills, B., Costa, A., Marigheto, N., & Wright, K. (2005). T-1-T-2 NMR correlation studies of high-pressure-processed starch and potato tissue. *Applied Magnetic Resonance, 28*(1–2), 13–27.

Hoseney, R. C. (1994). Back to the basics—bread baking. *Cereal Foods World, 39*(3), 180–183.

Jenkins, P. J., & Donald, A. M. (1995). The influence of amylose on starch granule structure. *International Journal of Biological Macromolecules, 17*(6), 315–321. doi:10.1016/0141-8130(96)81838-1.

Jenkins, P. J., & Donald, A. M. (1998). Gelatinisation of starch: a combined SAXS/WAXS/DSC and SANS study. *Carbohydrate Research, 308*(1–2), 133–147. doi:10.1016/s0008-6215(98)00079-2.

Kontogiorgos, V. (2011). Microstructure of hydrated gluten network. *Food Research International, 44*(9), 2582–2586. doi:10.1016/j.foodres.2011.06.021.

Le Botlan, D., Rugraff, Y., Martin, C., & Colonna, P. (1998). Quantitative determination of bound water in wheat starch by time domain NMR spectroscopy. *Carbohydrate Research, 308*(1–2), 29–36. doi:10.1016/s0008-6215(98)00068-8.

Le Grand, F., Cambert, M., & Mariette, F. (2007). NMR signal analysis to characterize solid, aqueous, and lipid phases in baked cakes. *Journal of Agricultural and Food Chemistry, 55*(26), 10947–10952. doi:10.1021/jf071735r.

Leach, H., Cowen, L., & Schoch, T. (1961). Structure of the starch granule. II Action of various amylases on granular starches. *Cereal Chemistry, 36*, 534–544.

Leon, A., Rosell, C. M., & de Barber, C. B. (2003). A differential scanning calorimetry study of wheat proteins. *European Food Research and Technology, 217*(1), 13–16. doi:10.1007/s00217-003-0699-y.

Luyts, A., Wilderjans, E., Waterschoot, J., Van Haesendonck, I., Brijs, K., Courtin, C. M., et al. (2013). Low resolution H-1 NMR assignment of proton populations in pound cake and its polymeric ingredients. *Food Chemistry, 139*(1–4), 120–128. doi:10.1016/j.foodchem.2013.01.062.

MacRitchie, F. (1976). The liquid-phase of dough and its role in baking. *Cereal Chemistry, 53*(3), 318–326.

Mariette, F., Davenel, A., Marchal, P., & Chaland, B. (1998). A study of water by NMR and MRI in dairy processes. *Revue de l'Institut Francais du Petrole, 53*(4), 521–525.

Marquardt, D.W. (1979). Algorithm for least-squares estimation of non-linear parameters. *Current Contents/Engineering Technology & Applied Sciences* (27), 14–14.

Meiboom, S., & Gill, D. (1958). Modified spin-echo method for measuring nuclear-relaxation times. *Current Contents/Engineering Technology & Applied Sciences* (38), 16–16.

Miller, R. A., & Hoseney, R. C. (2008). Role of salt in baking. *Cereal Foods Word, 53*(1), 4–6.

Ollett, A. L., Kirby, A. R., Clark, S. A., Parker, R., & Smith, A. C. (1993). The effect of water-content on the compaction behavior of potato starch. *Starch-Starke, 45*(2), 51–55. doi:10.1002/star.19930450205.

Ritota, M., Gianferri, R., Bucci, R., & Brosio, E. (2008). Proton NMR relaxation study of swelling and gelatinisation process in rice starch-water samples. *Food Chemistry, 110*(1), 14–22. doi:10.1016/j.foodchem.2008.01.048.

Roudaut, G., Farhat, I., Poirier-Brulez, F., & Champion, D. (2009). Influence of water, temperature and sucrose on dynamics in glassy starch-based products studied by low field H-1 NMR. *Carbohydrate Polymers, 77*(3), 489–495. doi:10.1016/j.carbpol.2009.01.029.

Rugraff, Y. L., Desbois, P., & LeBotlan, D. J. (1996). Quantitative analysis of wheat starch water suspensions by pulsed NMR spectroscopy measurements. *Carbohydrate Research, 295*, 185–194. doi:10.1016/s0008-6215(96)90140-8.

Steeneken, P. A. M. (1989). Rheological properties of aqueous suspensions of swollen starch granules. *Carbohydrate Polymers, 11*(1), 23–42. doi:10.1016/0144-8617(89)90041-6.

Tananuwong, K., & Reid, D. S. (2004). DSC and NMR relaxation studies of starch-water interactions during gelatinization. *Carbohydrate Polymers, 58*(3), 345–358. doi:10.1016/j.carbpol.2004.08.003.

Tang, H. R., Godward, J., & Hills, B. (2000). The distribution of water in native starch granules—a multinuclear NMR study. *Carbohydrate Polymers, 43*(4), 375–387. doi:10.1016/s0144-8617(00)00183-1.

Tang, H. R., Brun, A., & Hills, B. (2001). A proton NMR relaxation study of the gelatinisation and acid hydrolysis of native potato starch. *Carbohydrate Polymers, 46*(1), 7–18. doi:10.1016/s0144-8617(00)00265-4.

Uthayakumaran, S., Batey, I. L., Day, L., & Wrigley, C. W. (2011). Salt reduction in wheat-based foods—technical challenges and opportunities. *Food Australia, 63*(4), 137–140.

Wang, X., Choi, S. G., & Kerr, W. L. (2004). Water dynamics in white bread and starch gels as affected by water and gluten content. *Lebensmittel-Wissenschaft Und-Technologie-Food Science and Technology, 37*(3), 377–384. doi:10.1016/j.lwt.2003.10.008.

Wilhoft, E. M. (1973). Mechanism and theory of staling of bread and baked goods. And associated changes in textural properties. *Journal of Texture Studies, 4*, 292–322.

Zhu, W. X., Gayin, J., Chatel, F., Dewettinck, K., & Van der Meeren, P. (2009). Influence of electrolytes on the heat-induced swelling of aqueous dispersions of native wheat starch granules. *Food Hydrocolloids, 23*(8), 2204–2211. doi:10.1016/j.foodhyd.2009.05.002.